Cosmic Birefringence from the Axiverse

Silvia Gasparotto (IFAE)

Based on 2306.16355 with
Evangelos Sfakianakis

Axion++ 2023
Annecy 27/9/2023

What's *Cosmic Birefringence*?

Carroll, Field & Jackiw(1990); Harari & Sikivie (1992); Carroll (1998)

Uniform rotation of the polarization plane of the CMB photons

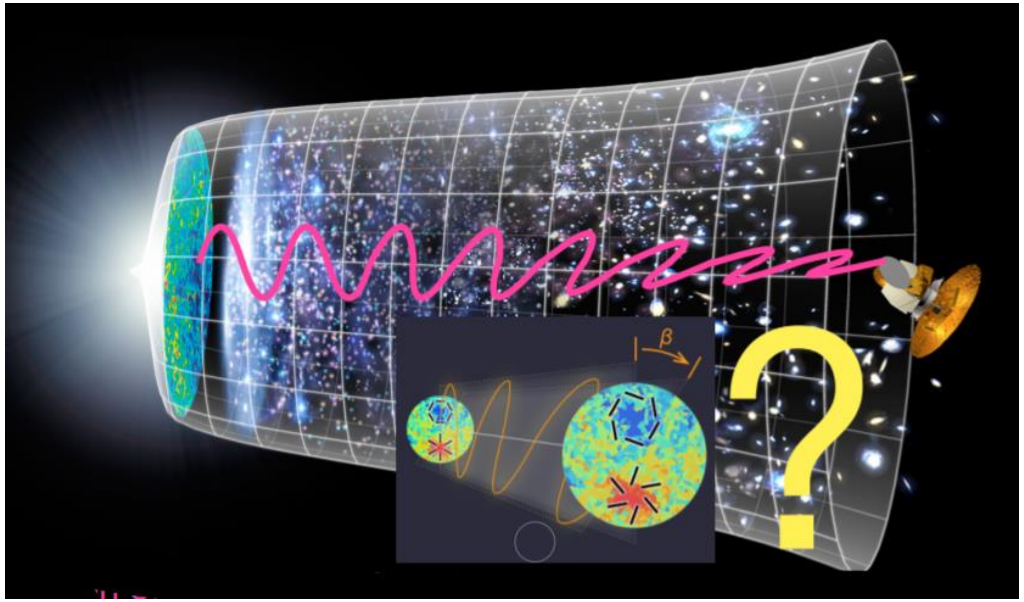

E and B are the CMB polarization states (Stokes)

*Signal of a **parity-violating** interaction in the electromagnetic sector.*

It shows up in the parity-odd power spectra of CMB

$$C_l^{EB,obs} = \frac{1}{2}\sin(4\beta)\left(C_l^{EE} - C_l^{BB}\right) + \cancel{C_l^{EB}}\cos(4\beta)$$

=0 in standard scenario

β is the angle of rotation

→ *degenerate with a miscalibration angle*

Minami and Komatsu (2020) developed a new method to measure β and the miscalibration angle simultaneously → $\beta = 0.35 \pm 0.14$ deg

Hint of Parity-Violating physics: Axions

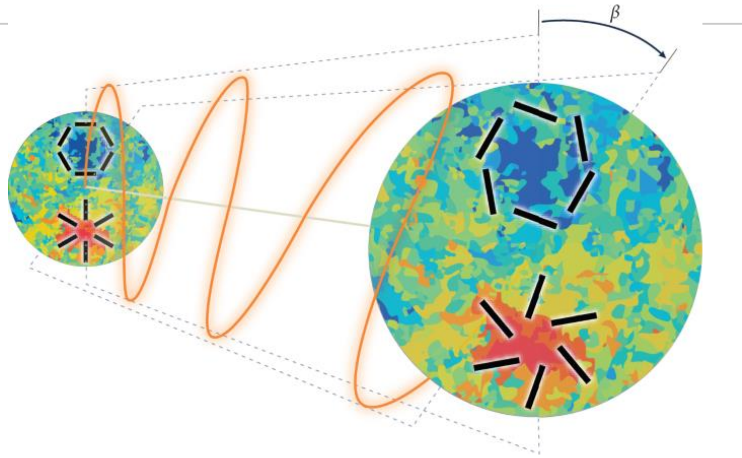

$\beta = 0.342^{+0.094}_{-0.091}\text{deg}\ (3.6\sigma)$ *Eskilt & Komatsu (2022)*

Zero is excluded at 99.987% C.L. , $\beta \propto \nu^n \rightarrow n = -0.35^{+0.48}_{-0.47}$

compatible with frequency independent signal

With the increase of sensibility, the confidence of detection is also increasing!

AXIONS can produce such a signal!

$$\mathcal{L}_{int} \ni \frac{1}{4} g_{\phi\gamma}\phi F_{\mu\nu}\tilde{F}^{\mu\nu} \rightarrow g_{\phi\gamma}\phi \vec{E}\cdot\vec{B}$$ *Parity-odd term*

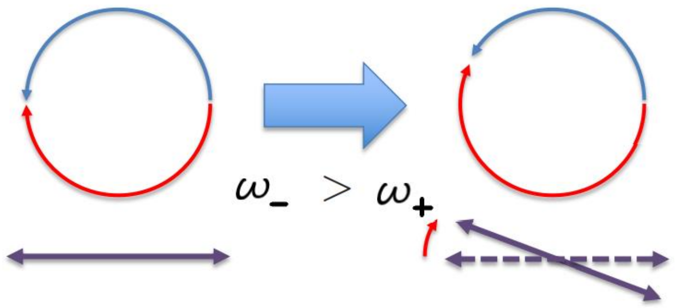

Modification of the Maxwell equations →
Left and Right-handed photons propagate with a different speed:

$$A''_\pm(\eta,k) + \underbrace{k^2\left(1 \mp \frac{g_{\phi\gamma}\phi'}{k}\right)}_{\omega^2_\pm} A_\pm(\eta,k) = 0$$

At first order: $\omega_\pm \simeq k \mp \frac{g_{\phi\gamma}}{2}\phi'$

- *Frequency independent*
- $\phi' \neq 0$

Birefringence angle and axion parameter space

$$\beta(\hat{n}) = \frac{1}{2}\int_{\eta_{em}}^{\eta_{obs}} d\eta(\omega_- - \omega_+) = \frac{g_{\phi\gamma}}{2}\int_{\eta_{em}}^{\eta_{obs}} d\eta\frac{d\phi}{d\eta} = \frac{g_{\phi\gamma}}{2}\left(\phi_{obs}(\hat{n}) - \phi_{em}(\hat{n})\right)$$

Axion-photon coupling *Field displacement*

T. Fujita et al. (2020)

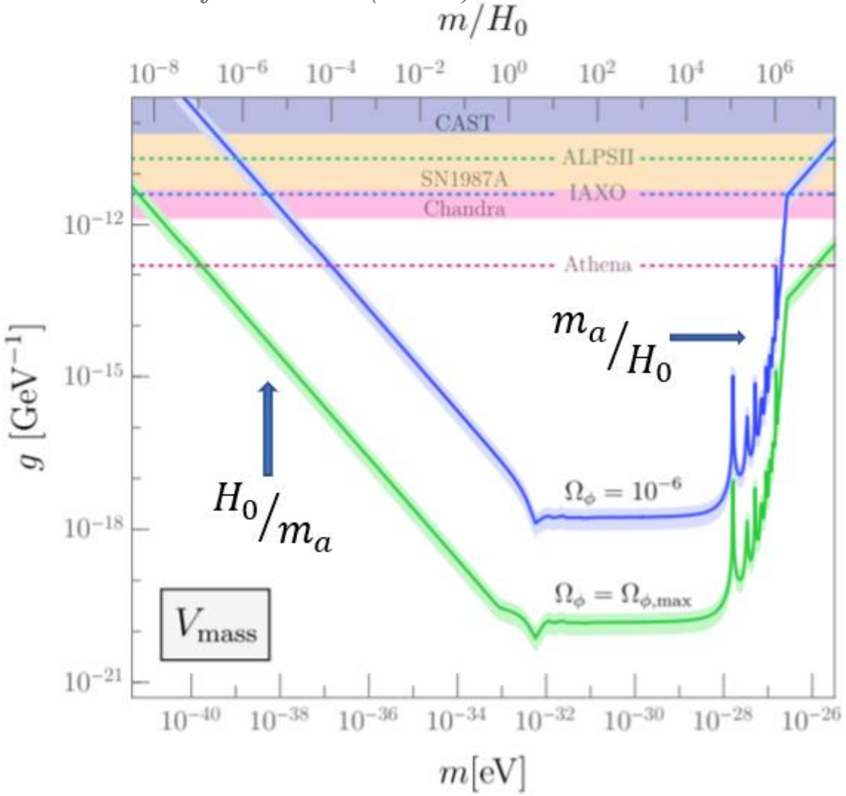

$$g_{\phi\gamma} = \frac{2\beta}{\Delta\phi}$$

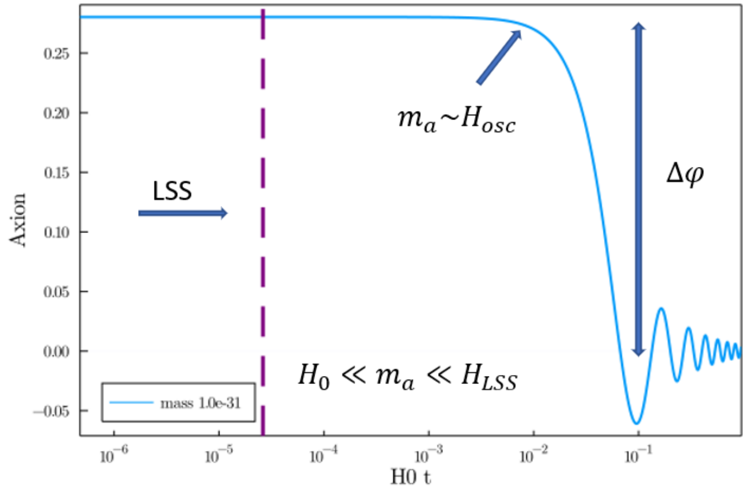

Take-home message: Axions within 15 orders of magnitude could explain the same signal → AXIVERSE*

Signal maximized for $10^{-33}eV \leq m_a \leq 10^{-29}eV$

String Axiverse

Arvanitaki, Dimopoulos, Dubovsky, Kaloper, March-Russell (2009)

Mehta et al (2021)

String Theory predicts many axions distributed over many orders of magnitude in mass and decay constant around GUT scale:

This discussion then suggests the following scenario for the distribution of f_a and m for different axions. The values of f_a are inversely proportional to the area of the corresponding cycle, so they do not change much from one axion to another. Given that the compactification is such that $S \gtrsim 200$ for string contributions to the QCD axion, and no special fine tuning is allowed, *all* axion decay constants in this scenario are likely to be close to the GUT scale $M_{GUT} \simeq 2 \times 10^{16}$ GeV. On the other hand, axion masses are exponentially sensitive to the area of the cycles, so that we expect their values to be homogeneously distributed on a log scale. Given that, as argued above, one can expect several hundred different cycles this suggests that there may be several string axions per decade of energy. It has also been argued recently that the mixing of axions

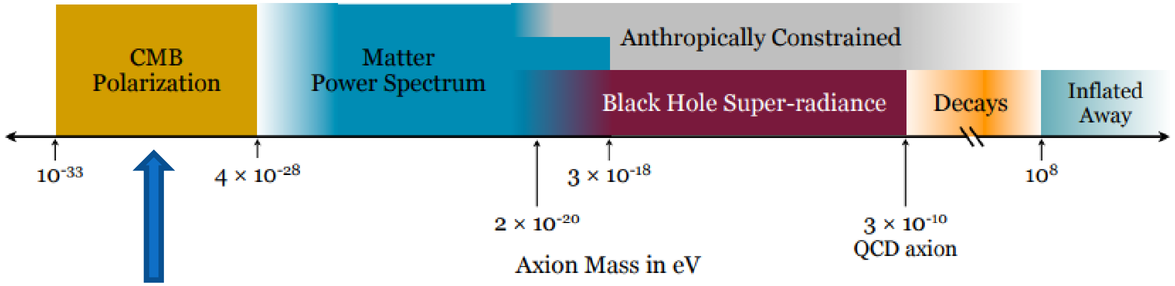

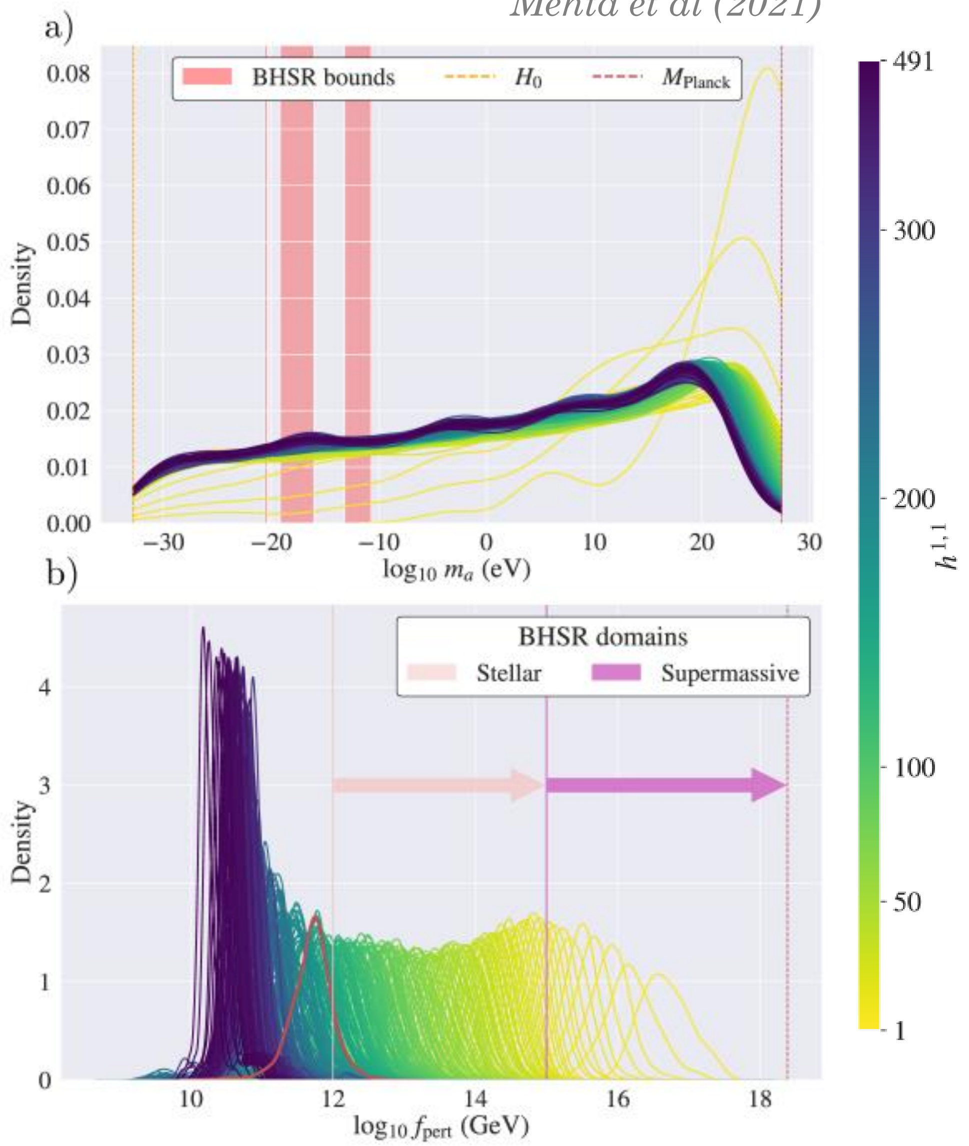

Emergent PDFs for the mass and the decay constant

Toy Model: Cosine Potential

Cosmic Birefringence

$$\beta = \sum_{i=0}^{N} \frac{\alpha_{em}}{2\pi f_{a,i}} \frac{\phi_{in,i}}{2} \quad \text{with} \quad g_{\phi\gamma,i} = \frac{\alpha_{em}}{2\pi f_{a,i}}$$

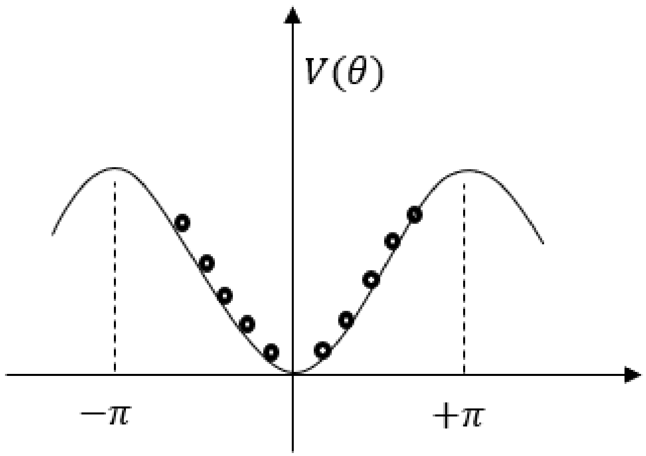

With uniform initial conditions $\theta_i = \frac{\phi_i}{f_{a,i}} \in [-\pi, \pi]$

$\langle\beta\rangle = 0$ *the mean is zero,*

but the VARIANCE grows with $\sqrt{N}$

$$\sqrt{\langle\beta^2\rangle} = \frac{\alpha_{em}}{4\pi}\sqrt{\sum_{i=1}^{N} \vartheta_i^2} = 0.06\sqrt{N}\, deg \quad \rightarrow \beta \sim 0.3\, deg$$

$$N(10^{-33} eV \leq m_a \leq 10^{-29} eV) = 25 \quad \rightarrow N_{dec} = 6$$

Statistical treatment of β *is ok!*

Note: $N_{tot} \simeq N_{dec} \times \log\frac{m_{max}}{m_{min}} = 6 \times \log\frac{M_{pl}}{H_0} = 360$

This is assuming no mixing between different axions and $c_i \sim 1\ldots$

We move to the quadratic potential and then consider the Monodromy potential

Probability distributions of m_a, f_a, ϕ_{in}

- *Initial field value follows a Gaussian distribution $N(0, \sigma_\phi)$ with $\sigma_\phi \sim H_{inf}$*

- *Decay constant follows a log-normal distribution*

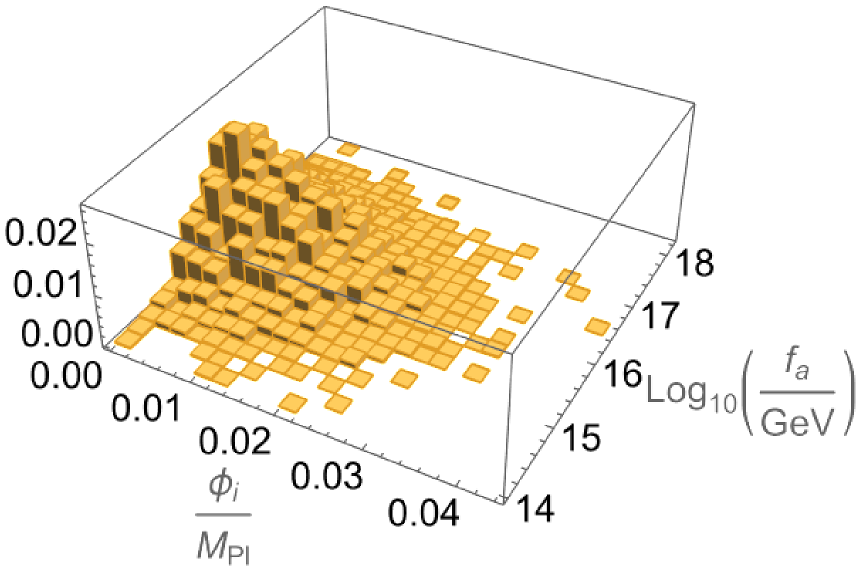

Mehta et al (2021)

- *Probability density function (PDF) of the mass within $H_0 \leq m_a \leq M_{Pl}$*

  → almost flat at very low masses

- *Presence of correlations between model parameters*

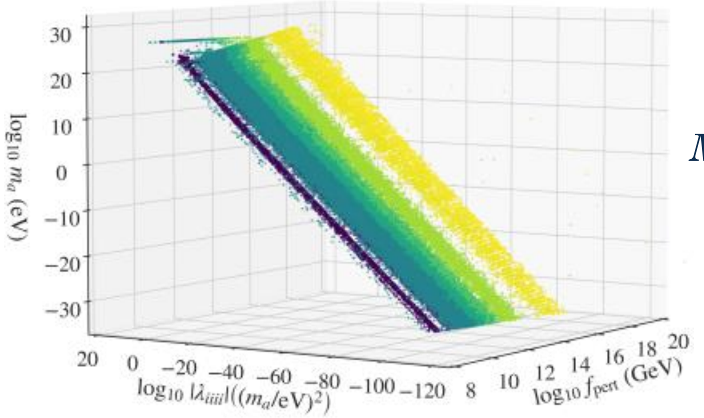

Emergent correlation between Mass and decay constant $\rho(m_a, f_a) \sim 0.5$

Implications for the Quadratic Potential

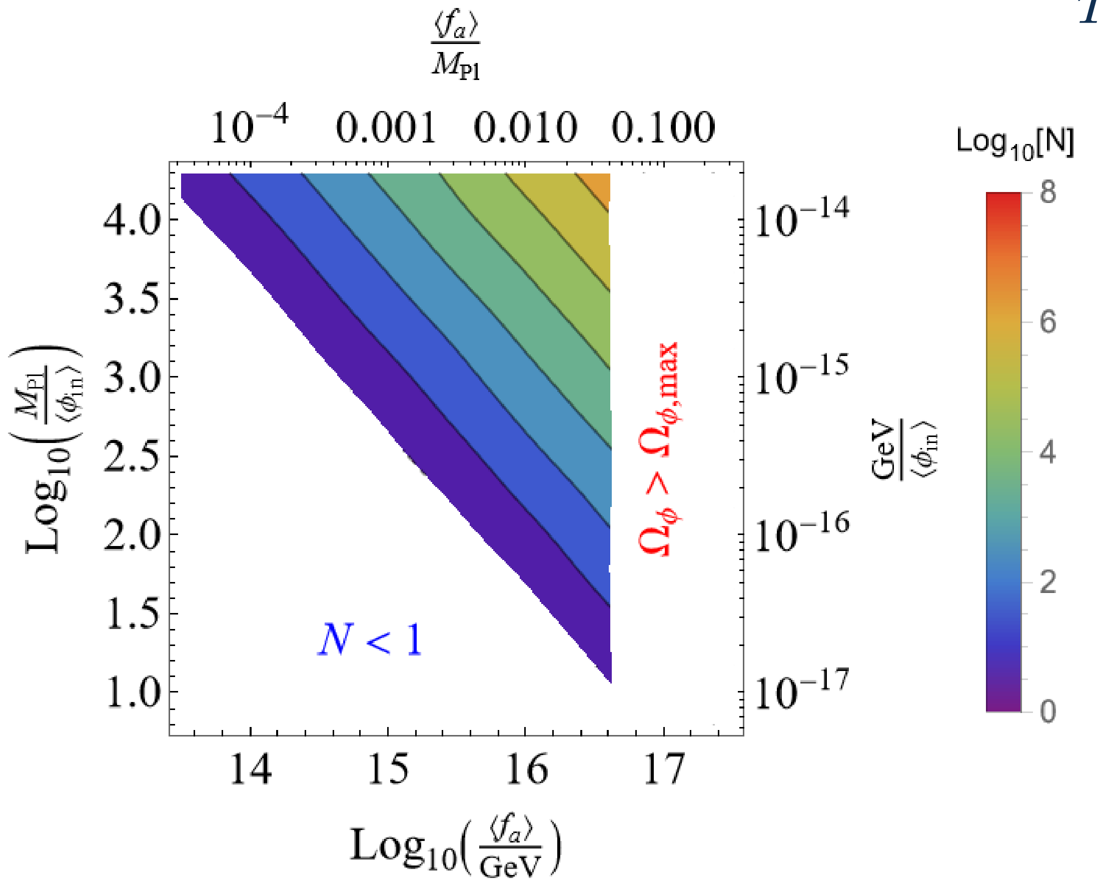

The constraint comes from the different scaling of β and Ω_ϕ

$$\beta \approx \sigma_\beta \approx 0.033 \sqrt{N} \frac{\sigma_\phi}{\langle f_a \rangle}\, deg$$

Enforcing $\beta \sim 0.3\ deg,\ N \sim 100 \left(\frac{\langle f_a \rangle}{\sigma_\phi}\right)^2$

Inserting into the axion abundance:

$$\Omega_\phi \cong \frac{3}{8} \frac{\sigma_\phi^2}{M_{pl}^2} \sum_{i=1}^{N} \frac{\phi_{in}^2}{\sigma_\phi^2} \cong \frac{3}{8} \frac{\sigma_\phi^2}{M_{pl}^2} N \sim \frac{75}{2} \left(\frac{\langle f_a \rangle}{M_{pl}}\right)^2$$

Asking $\Omega_\phi \leq \Omega_{\phi,max}$ a few percent of DM gives an upper bound on the decay constant!

Implications for the Quadratic Potential

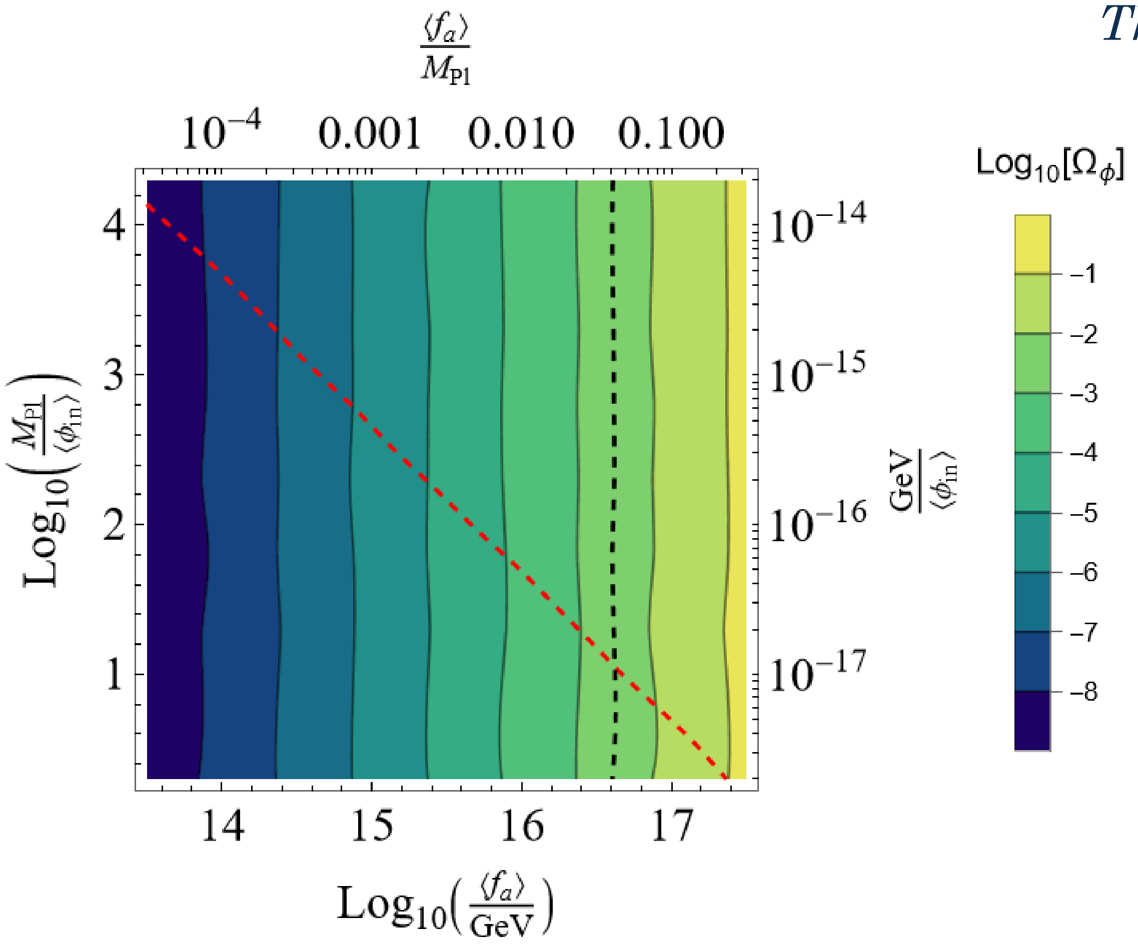

The constraint comes from the different scaling of β and Ω_ϕ

$$\beta \approx \sigma_\beta \approx 0.033\sqrt{N}\frac{\sigma_\phi}{\langle f_a \rangle}\, deg$$

Enforcing $\beta \sim 0.3$ deg, $N \sim 100\left(\frac{\langle f_a \rangle}{\sigma_\phi}\right)^2$

Inserting into the axion abundance:

$$\Omega_\phi \cong \frac{3}{8}\frac{\sigma_\phi^2}{M_{pl}^2}\sum_{i=1}^{N}\frac{\phi_{in}^2}{\sigma_\phi^2} \cong \frac{3}{8}\frac{\sigma_\phi^2}{M_{pl}^2} N \sim \frac{75}{2}\left(\frac{\langle f_a \rangle}{M_{pl}}\right)^2$$

Asking $\Omega_\phi \leq \Omega_{\phi,max}$ a few percent of DM gives an upper bound on the decay constant!

Projecting the abundance at higher masses

With just the Birefringence we cannot test the mass distribution at masses $m_a \geq 10^{-28} eV \sim H_{eq}$ *, but assuming the same distribution on* f_a *and* ϕ_{in} *at higher masses*

$$\langle \Omega_{\phi,tot} \rangle = \frac{N}{6}(9\Omega_r)^{\frac{3}{4}} \left\langle \sqrt{\frac{m}{H_o}} \right\rangle \left\langle \left(\frac{\phi_{in}}{M_{Pl}} \right)^2 \right\rangle$$

$$\rightarrow \frac{N_{dec}}{3log(10)}(9\Omega_r)^{\frac{3}{4}} \sqrt{\frac{m_{max}}{H_0}} \frac{\sigma_{phi}^2}{M_{Pl}^2} \quad with \;\; N_{dec} \sim 25 \left(\frac{\langle f_a \rangle}{\sigma_\phi} \right)^2$$

$$\langle \Omega_{\phi,tot} \rangle \rightarrow \frac{25(9\Omega_r)^{\frac{3}{4}}}{3log(10)} \sqrt{\frac{m_{max}}{H_0} \frac{\langle f_a \rangle^2}{M_{Pl}^2}}$$

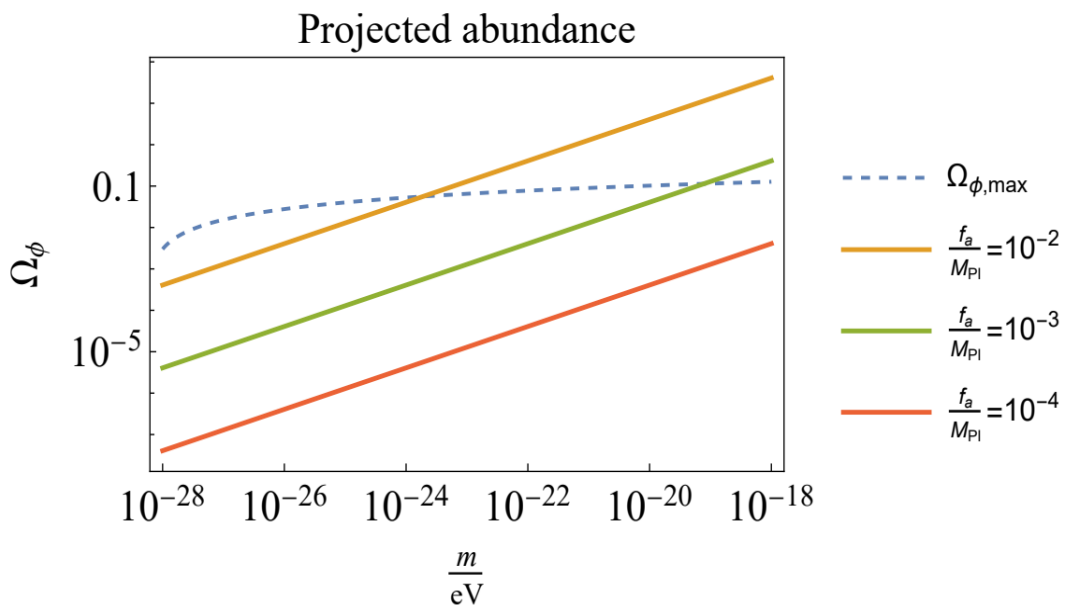

Comparing it with the current bounds on Ω_{phi} *we find* m_{max} *that depends on* $\langle f_a \rangle$*!*

Testing the Mass Distribution with Birefringence Tomography

The β-angle is only approximately constant, l-dependence comes from the contribution at different epochs:

1. *Recombination* $z \sim 1000 \rightarrow m_a \leq 3 \times 10^{-29}\ eV$
2. *Reionization* $z \sim 8 \rightarrow m_a \leq 10^{-31}\ eV$

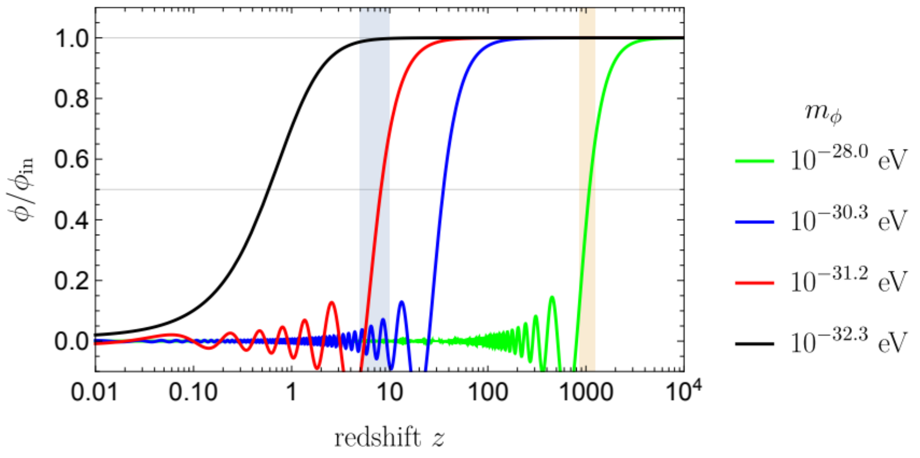

Reionization bump can probe $10^{-32} \leq m_a \leq 10^{-31}\ eV$:

$$\frac{\beta_{rei}}{\beta_{rec}} \cong \frac{\sqrt{N_{tot} P(10^{-32} \leq m_a \leq 10^{-31}\ eV)}}{\sqrt{N_{tot} P(10^{-33} \leq m_a \leq 10^{-29}\ eV)}} \cong \frac{\sqrt{2}}{\sqrt{4}} \approx 0.7$$

Uniform mass distribution

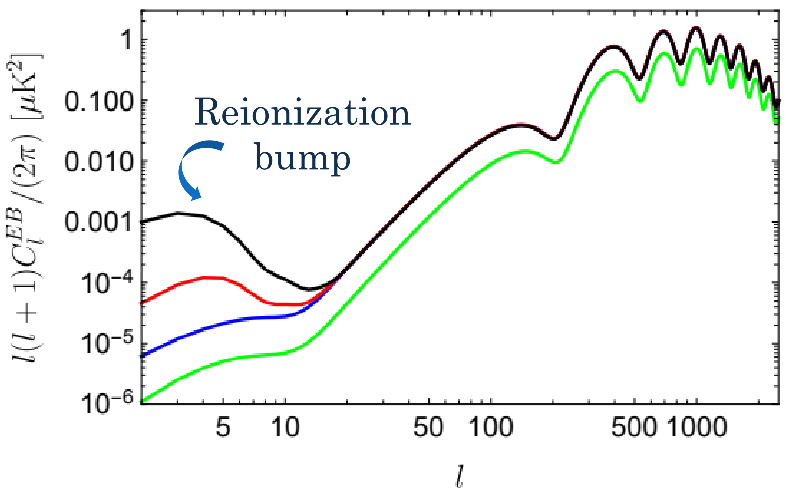

Hiromasa Nakatsuka et al. (2022)

Independent on the total number of axions across all masses!

Effect of correlations: mass and decay constant

The presence of correlations weights differently the contribution from different axions:

- $\rho(m_a, f_a) > 0 \rightarrow$ *contribution from heavier axions is suppressed* $\beta_{rec} \sim \beta_{rei}$
- $\rho(m_a, f_a) < 0 \rightarrow$ *contribution from lighter axions is suppressed* $\beta_{rec} \gg \beta_{rei}$

This changes the emergent distribution of β_{rei}/β_{rec}

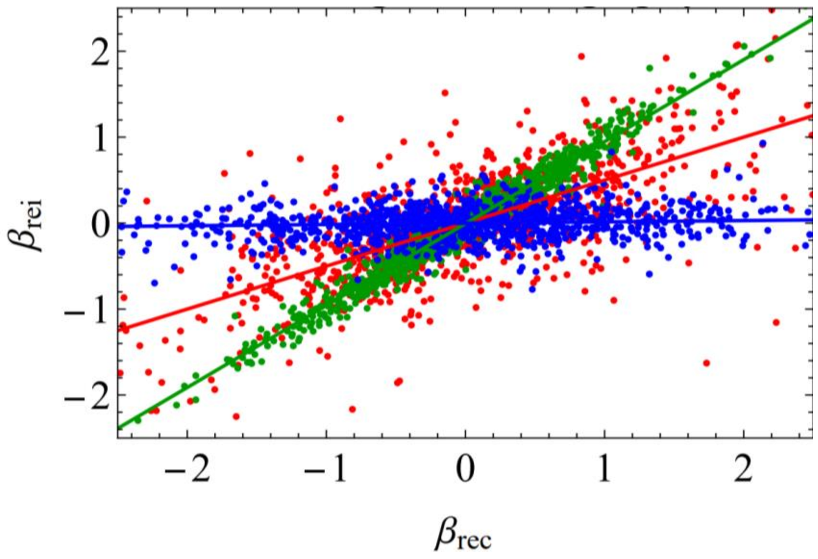

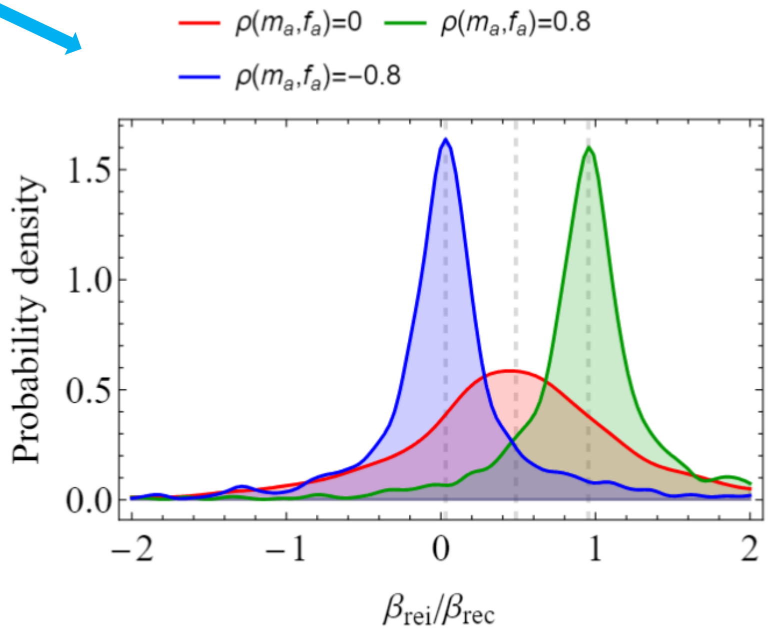

Conclusions

- *The signal can be explained with several axions per decade* $\rightarrow$ *depending on* ϕ_{in} *and* f_a

- *The axion abundance sets a general bound on* $f_a \leq 10^{17}$ *GeV, the bound changes by:*

  $O(1)$ *in the presence of correlation* $\rho(f_a, \phi_{in})$

  $O(10)$ *for the Monodromy potential*

- *Expectation at higher masses of the abundance suggests a link between* m_{max} *and* $\langle f_a \rangle$
  $\rightarrow m_{max} \sim 10^{-24} eV$ *for* $\langle f_a \rangle \sim 10^{16} GeV$

- *Birefringence tomography will allow testing Axiverse PDFs*

  $\rightarrow$ *mass distribution and presence of correlations* $\rho(m_a, f_a, \phi_{in})$

Cosmic birefringence as a complementary test for the Axiverse at lower masses (lower than those accessible to Superradiance)

Thank you for your attention!

sgasparotto@ifae.es

Aligned case

The expectation changes if the initial value is not randomly distributed around zero but it has a preferable sign.

In this case $\langle\beta\rangle \approx 0.033\, N \frac{\langle\phi_{in}\rangle}{\langle f_a\rangle}\, deg \rightarrow N \sim 10 \frac{\langle f_a\rangle}{\langle\phi_{in}\rangle}$

Thus the abundance gives

$$\Omega_\phi \cong \frac{3}{8} N \left(\frac{\langle\phi_{in}\rangle^2}{M_{pl}^2} + \frac{\sigma_\phi^2}{M_{pl}^2} \right) \sim \frac{30}{8} \frac{\langle f_a\rangle}{\langle\phi_{in}\rangle} \left(\frac{\langle\phi_{in}\rangle^2}{M_{pl}^2} + \frac{\sigma_\phi^2}{M_{pl}^2} \right)$$

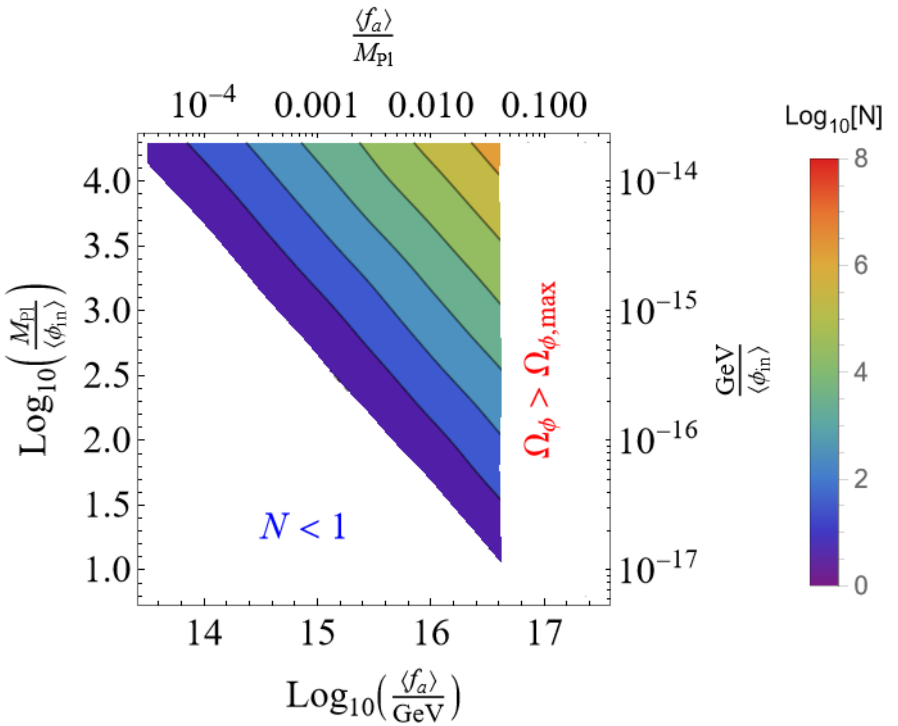

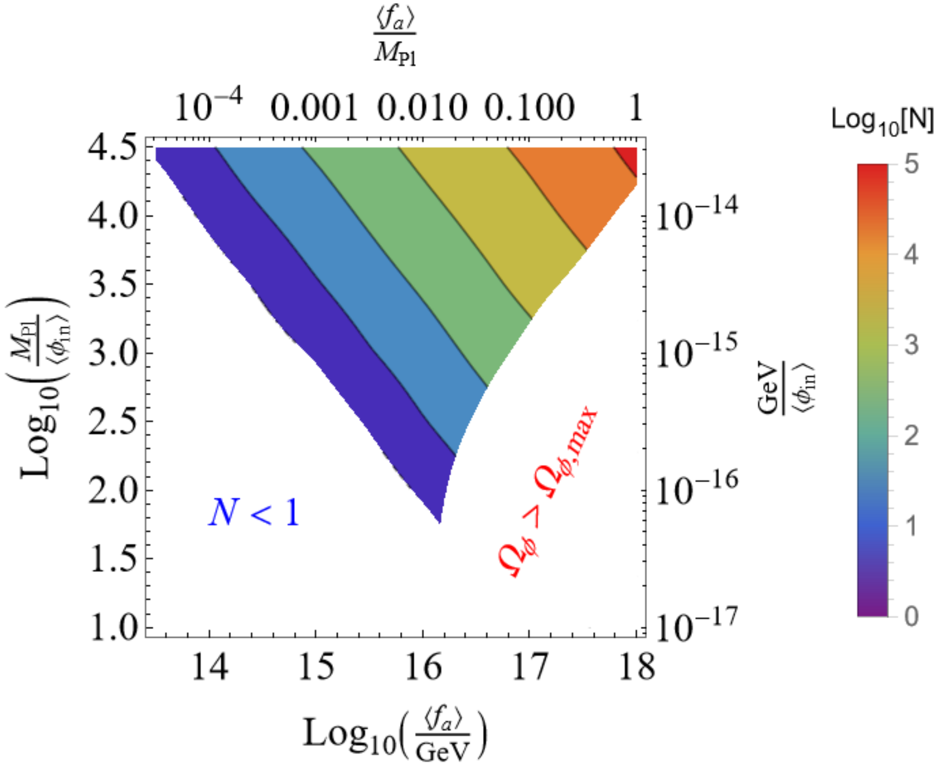

Aligned case

The expectation changes if the initial value is not randomly distributed around zero but it has a preferable sign.

In this case $\langle\beta\rangle \approx 0.033\, N \frac{\langle\phi_{in}\rangle}{\langle f_a\rangle}\, deg \rightarrow N \sim 10 \frac{\langle f_a\rangle}{\langle\phi_{in}\rangle}$

Thus the abundance gives

$$\Omega_\phi \cong \frac{3}{8} N \left(\frac{\langle\phi_{in}\rangle^2}{M_{pl}^2} + \frac{\sigma_\phi^2}{M_{pl}^2}\right) \sim \frac{30}{8}\frac{\langle f_a\rangle}{\langle\phi_{in}\rangle}\left(\frac{\langle\phi_{in}\rangle^2}{M_{pl}^2} + \frac{\sigma_\phi^2}{M_{pl}^2}\right)$$

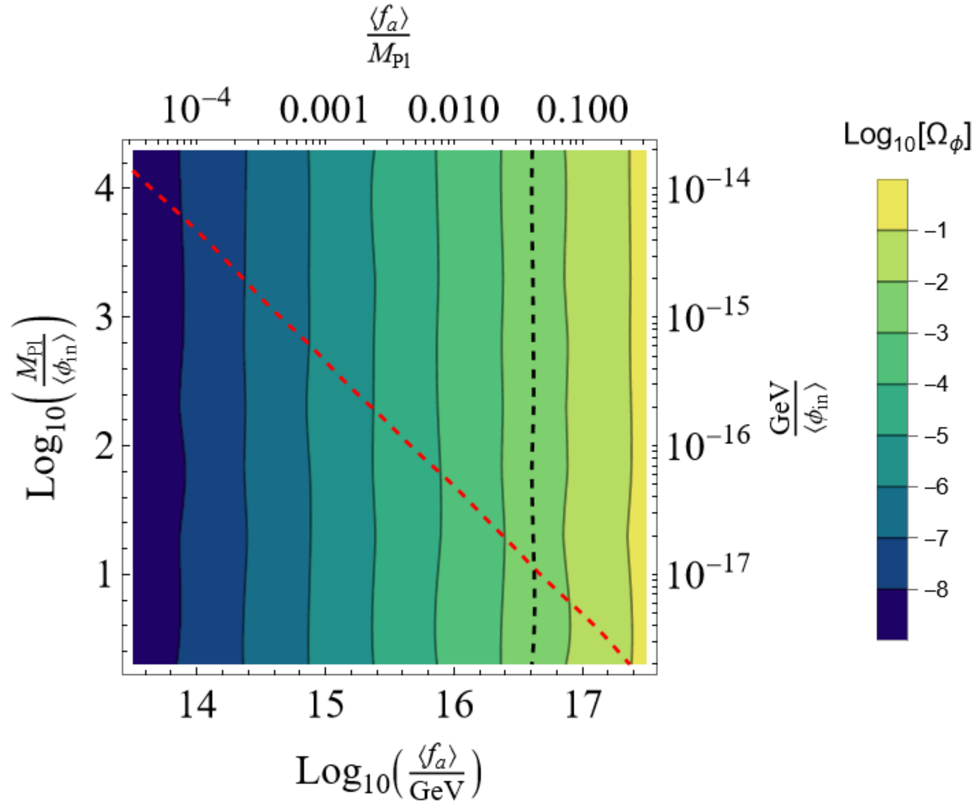

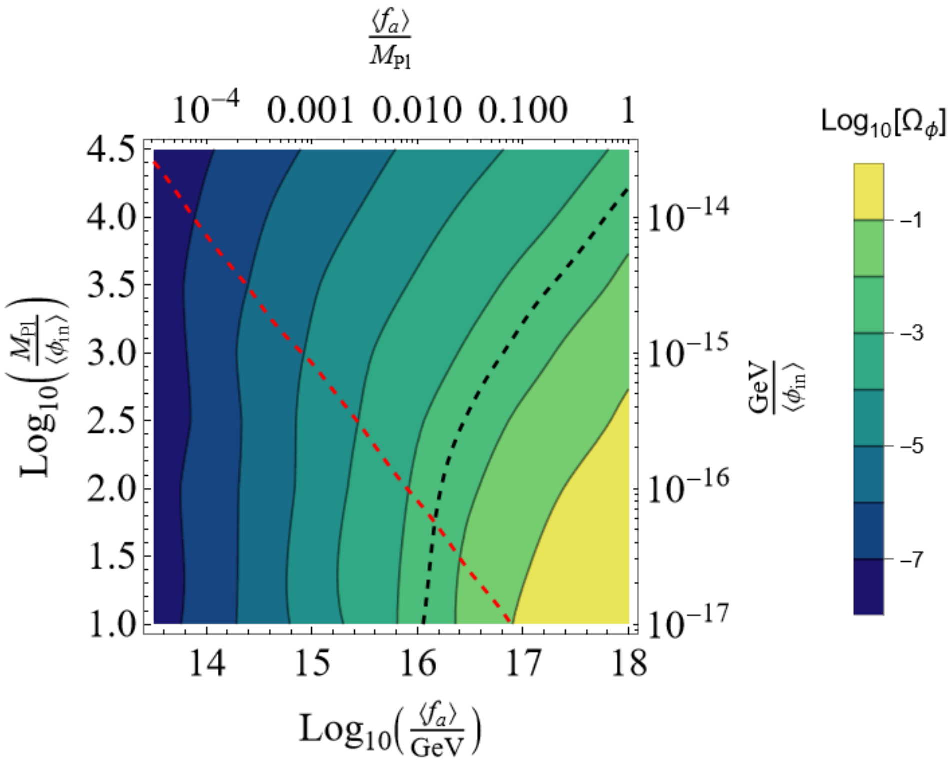

Monodromy potential

Monodromy potential, asymptotically flat at large field values

$$V(\phi) = \frac{M^2 m^2}{2p}\left[\left(1+\frac{\phi^2}{M^2}\right)^p - 1\right] \qquad p = \frac{1}{2}$$

The results change depending on the

initial condition ϕ_i, the mass m and the transition scale M,

Three types of evolution: linear potential, quadratic potential and transition of behavior

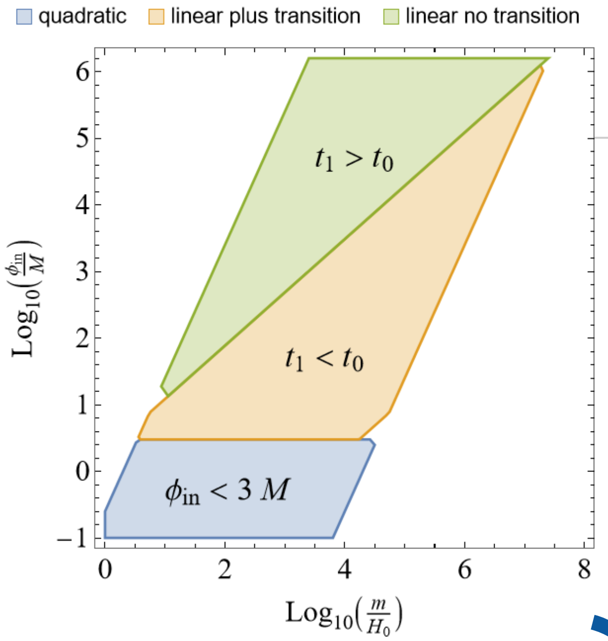

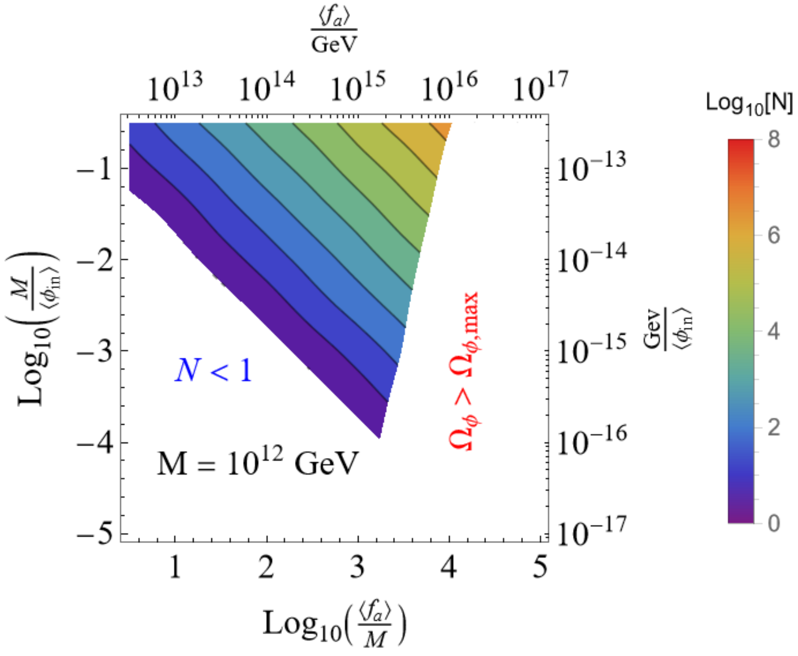

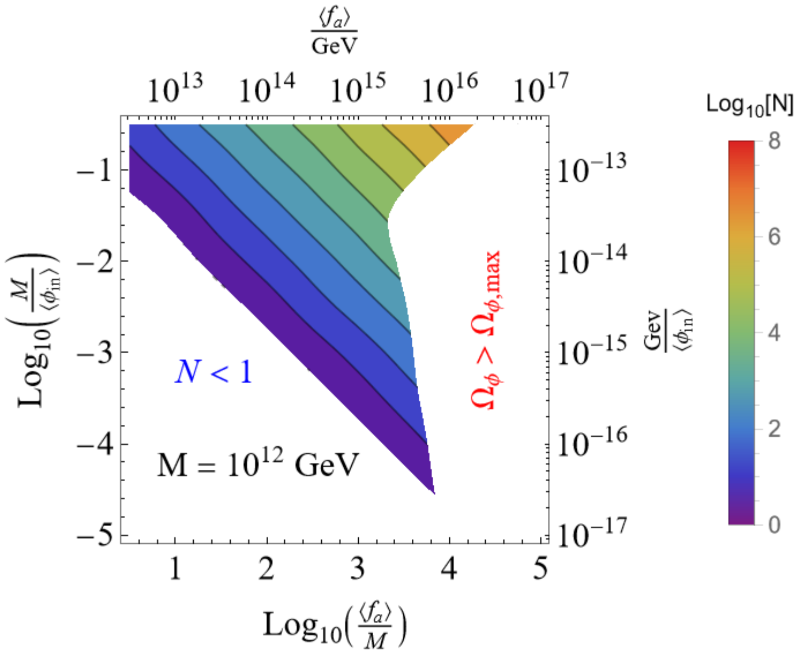

In each region the final abundance has a different dependence on the model parameters → different bound on the (f_a, ϕ_{in}) plane